

# Bose-Einstein condensate in a harmonic trap decorated with Dirac $\delta$ functions

Haydar Uncu<sup>1</sup>, Devrim Tarhan<sup>2</sup>, Ersan Demiralp<sup>1,3</sup>, Özgür E. Müstecaplıoğlu<sup>4</sup>

<sup>1</sup>*Department of Physics, Boğaziçi University, Bebek, 34342, İstanbul, Turkey*

<sup>2</sup>*Department of Physics, Harran University, Osmanbey Yerleşkesi, Şanlıurfa, Turkey*

<sup>3</sup>*Boğaziçi University-TÜBİTAK Feza Gürsey Institute Kandilli, 81220, İstanbul, Turkey and*

<sup>4</sup>*Department of Physics, Koç University Rumelifeneri yolu, Sarıyer, 34450, İstanbul, Turkey*

(Dated: July 6, 2018)

We study Bose-Einstein condensation in a harmonic trap with a dimple potential. We specifically consider the case of a tight and deep dimple potential which is modelled by a Dirac  $\delta$  function. This allows for simpler, explicit numerical and analytical investigations of noninteracting gases. Thus, the Schrödinger equation is used instead of the Gross-Pitaevski equation. Calculating the atomic density, chemical potential, critical temperature and condensate fraction, the role of the relative depth of the dimple potential with respect to the harmonic trap in large condensate formation at enhanced temperatures is clearly revealed.

PACS numbers: 03.75.Hh, 03.65.Ge

## I. INTRODUCTION

Bose-Einstein condensation was the last major discovery of Einstein [1, 2]. By applying the Bose-Einstein statistics to an ideal gas, Einstein showed that “from a certain temperature on, the molecules condense without attractive forces ...” [3] and discovered the Bose-Einstein condensation in 1925. This theoretical prediction motivated the experimental studies for realizations of Bose-Einstein condensates of gases. Seventy years after the prediction of Einstein, Bose-Einstein condensates (BEC) of dilute gases have been observed at very low temperatures by using ingenious experimental designs [4, 5, 6].

Experimentally available condensates are systems with finite number of atoms  $N$ , confined in spatially inhomogeneous trapping potentials. Their understanding requires theories that go beyond the usual treatments based upon London’s continuous spectrum approximation [7] or the thermodynamic limit  $N \rightarrow \infty$ . Such studies [8, 9] reveal that BEC can occur in harmonically trapped lower-dimensional systems for finite  $N$  despite the enhanced importance of phase fluctuations [10]. Quasicondensates with large phase fluctuations may still occur [11]. This is in contrast to standard results [12], in agreement with the Mermin-Wagner-Hohenberg theorem [13, 14] in the thermodynamic limit. Bose-Einstein condensation in one dimension (1D) with a harmonic trap is attractive due to enhanced critical temperature and condensate fraction [8, 9]. Recently, one- and two- dimensional BECs have been created in experiments [15]. One-dimensional condensates were also generated on a microchip [16, 17] and in lithium mixtures [18].

Modification of the shape of the trapping potential can be used to increase the phase space density [19]. “Dimple”-type potentials are the most favorable potentials for this purpose [20, 21, 22]. The phase-space density can be enhanced by an arbitrary factor by using a small dimple potential at the equilibrium point of the harmonic trapping potential [20]. A recent demonstration of caesium BEC exploits a tight dimple poten-

tial [21]. Quite recently, such potentials were proposed for efficient loading and fast evaporative cooling to produce large BECs [23]. Tight dimple potentials for one-dimensional (or strictly speaking quasi-one-dimensional) BECs offer attractive applications, such as controlling interaction between dark solitons and sound [24], introducing defects such as atomic quantum dots in optical lattices [25], or quantum tweezers for atoms [26]. Such systems can also be used for spatially selective loading of optical lattices [27]. In combination with the condensates on atom chips, tight and deep dimple potentials can lead to rich novel dynamics for potential applications in atom lasers, atom interferometers and in quantum computations (see Ref. [28] and references therein).

In this paper, we investigate Bose-Einstein condensation in a 1D harmonic trap decorated by a tight and deep dimple potential. The quantum kinetics of a similar system but for a 3D single-mode trap, modelled by a deep but narrow spherical square potential well, was studied in Ref. [29], where a master equation, to describe condensate growth, was developed. We model the dimple potential using a Dirac  $\delta$  function. The delta function can be defined via a Gaussian function [30]  $g(x, a) = (1/\sqrt{\pi}a) \exp(-x^2/a^2)$  of infinitely narrow width  $a$  so that  $g(x, a) \rightarrow \delta(x)$  for  $a \rightarrow 0$ . This allows for analytical calculations in some limiting cases as well as a simpler numerical treatment for arbitrary parameters. We calculate the transition temperature as well as the chemical potential and condensate fraction for various number of atoms and for various relative depths of the dimple potential. For describing a system with interacting particles, the Gross-Pitaevski equation is usually utilized. We note that we neglect the interactions between atoms in our model, and thus the Schrödinger equation for the harmonic trap with the dimple potential is solved.

The paper is organized as follows. In Sect. II, we present the analytical solutions of the Schrödinger equation for a Dirac  $\delta$ -decorated harmonic potential and the corresponding eigenvalue equation. In Sect. III, deter-

mining the eigenvalues numerically, we show the effect of the dimple potential on the condensate fraction and the transition temperature. In Sect. IV, we present a semi-classical method to calculate condensate fraction when a dimple potential is added to harmonic trap adiabatically. Analytical results in the limit of strong dimple potential are presented in the Sect. V. Finally, we present our conclusions in Sect. VI.

## II. HARMONIC POTENTIAL DECORATED WITH DIRAC DELTA FUNCTIONS

We begin our discussion with the one dimensional harmonic potential decorated with the Dirac  $\delta$  functions [31]-[33]. This potential is given as

$$V(x) = \frac{1}{2}m\omega^2 x^2 - \frac{\hbar^2}{2m} \sum_i^P \sigma_i \delta(x - x_i), \quad (1)$$

where  $\omega$  is the frequency of the harmonic trap,  $P$  is a finite integer, and  $\sigma_i$ 's are the strengths (depths) of the dimple potentials located at  $x_i$ 's with  $x_1 < x_2 < \dots < x_P$  with  $x_i \in (-\infty, \infty)$ . The factor  $\hbar^2/2m$  is used for calculational convenience. A negative  $\sigma_i$  value represents repulsive interaction while positive  $\sigma_i$  value represents attractive interaction. We can write time-independent Schrödinger equation as

$$-\frac{\hbar^2}{2m} \frac{d^2 \Psi(x)}{dx^2} + V(x) \Psi(x) = E \Psi(x). \quad (2)$$

By inserting  $E = (\xi + \frac{1}{2})\hbar\omega$ , with  $\xi$  a real number, and introducing dimensionless quantities  $z = x/x_0$ , and  $z_i = x_i/x_0$  with  $x_0 = \sqrt{\hbar/2m\omega}$ , the natural length scale of the harmonic trap, we can re-express Eq. (2) as

$$\frac{d^2 \Psi(z)}{dz^2} + \left[ \xi + \frac{1}{2} - \frac{z^2}{4} + \sum_i^P \Lambda_i \delta(z - z_i) \right] \Psi(z) = 0, \quad (3)$$

where  $\Lambda_i = x_0 \sigma_i$ . For  $z \neq z_i$ , the Eq. (2) has two linearly independent solutions. For  $\xi \neq 0, 1, 2, \dots$  these linearly independent solutions are parabolic cylinder functions  $D_\xi(z)$  and  $D_\xi(-z)$ , defined as:

$$D_\xi(z) = 2^{\frac{\xi}{2}} e^{-\frac{z^2}{4}} \times \left\{ \frac{\sqrt{\pi} \Phi\left(-\frac{\xi}{2}, \frac{1}{2}; \frac{z^2}{2}\right)}{\Gamma\left(\frac{1-\xi}{2}\right)} - \frac{\sqrt{2\pi} z \Phi\left(\frac{1-\xi}{2}, \frac{3}{2}; \frac{z^2}{2}\right)}{\Gamma\left(-\frac{\xi}{2}\right)} \right\} \quad (4)$$

$$D_\xi(-z) = 2^{\frac{\xi}{2}} e^{-\frac{z^2}{4}} \times \left\{ \frac{\sqrt{\pi} \Phi\left(-\frac{\xi}{2}, \frac{1}{2}; \frac{z^2}{2}\right)}{\Gamma\left(\frac{1-\xi}{2}\right)} + \frac{\sqrt{2\pi} z \Phi\left(\frac{1-\xi}{2}, \frac{3}{2}; \frac{z^2}{2}\right)}{\Gamma\left(-\frac{\xi}{2}\right)} \right\}, \quad (5)$$

where  $\Phi(-\xi/2, 1/2; z^2/2)$  and  $\Phi((1-\xi)/2, 3/2; z^2/2)$  are the confluent hypergeometric functions  $\Phi(a, b; z^2/2)$

defined in Ref. [34] for  $a = \xi/2$ ,  $b = 1/2$  and  $a = (1-\xi)/2$ ,  $b = 3/2$ , respectively. Thus, the general solution of Eq. (3) between the locations of two Dirac  $\delta$  functions is

$$\Psi(z) = a_i D_\xi(z) + b_i D_\xi(-z), \quad (6)$$

with  $a_i$  and  $b_i$  can be written in terms of  $b_1$  via transfer matrix method and  $b_1$  is determined by normalization ( $a_1 = b_{P+1} = 0$  due to square integrability) [33, 35].  $D_\xi(-z)$  is regular as  $z \rightarrow -\infty$ , but  $|D_\xi(-z)| \rightarrow +\infty$  as  $z \rightarrow \infty$ , and  $D_\xi(z)$  is regular as  $z \rightarrow \infty$ , but  $|D_\xi(z)| \rightarrow +\infty$  as  $z \rightarrow -\infty$  [34]. By using the transfer matrix method explained in Refs. [31, 35], one finds the eigenvalue equation for the potential given in Eq. (1). For the special case of the potential given in Eq. (1), harmonic potential decorated with one Dirac  $\delta$  function at its center  $P = 1$ ,  $x_1 = 0$ ,

$$V(x) = \frac{1}{2}m\omega^2 x^2 - \frac{\hbar^2}{2m} \sigma \delta(x), \quad (7)$$

the eigenvalue equation of the even states is written as [32, 33, 36]:

$$\frac{\Gamma((1-\xi)/2)}{\Gamma(-\xi/2)} = \frac{\Gamma(3/4 - E/2\hbar\omega)}{\Gamma(1/4 - E/2\hbar\omega)} = \frac{\sigma \sqrt{\hbar/m\omega}}{4}. \quad (8)$$

In this case, the odd solutions of the harmonic potential are unaffected because the Dirac  $\delta$  function is located at the center of the harmonic potential. On the other hand, the energy eigenvalues of even states change as a function of  $\sigma$ . The ground state energy eigenvalue decreases unlimitedly as  $\sigma$  increases (attractive case). However, the energies of the excited even states are limited by the energies  $E_{2n+1}$  of odd states and as  $\sigma \rightarrow \infty$ ,  $E_{2n+2} \rightarrow E_{2n+1} = (2n+1+1/2)\hbar\omega$  where  $n = 0, 1, \dots$ . Thus, as  $\sigma \rightarrow \infty$  the energy eigenvalues of these states go to the energy eigenvalue of the one lower eigenstate, and the odd energy eigenstates asymptotically become doubly degenerate.

## III. BEC IN A ONE-DIMENSIONAL HARMONIC POTENTIAL WITH A DIRAC $\delta$ FUNCTION

We begin our discussion about BEC in a one-dimensional harmonic potential decorated with a Dirac  $\delta$  function by investigating the change of the critical temperature as a function of  $\sigma$ . One estimates a  $\sigma$  value using the parameters of Ref.[22]. In this paper, the minimum value of the dimple potential is given as  $U_c = k_B 4 \mu\text{K}$  and average potential width is given as  $r = 1 - 100 \mu\text{m}$ . We equate the strength  $(-\hbar^2 \sigma / 2m)$  to the product  $U_c r$  to get an estimate of  $\sigma$ . We find that  $\sigma$  varies approximately between  $10^8$  1/m and  $10^{10}$  1/m as  $r$  changes from  $1 \mu\text{m}$  to  $100 \mu\text{m}$ . We define a dimensionless parameter in terms of  $\sigma$  as:

$$\Lambda = \sigma \sqrt{\frac{\hbar}{m\omega}}. \quad (9)$$

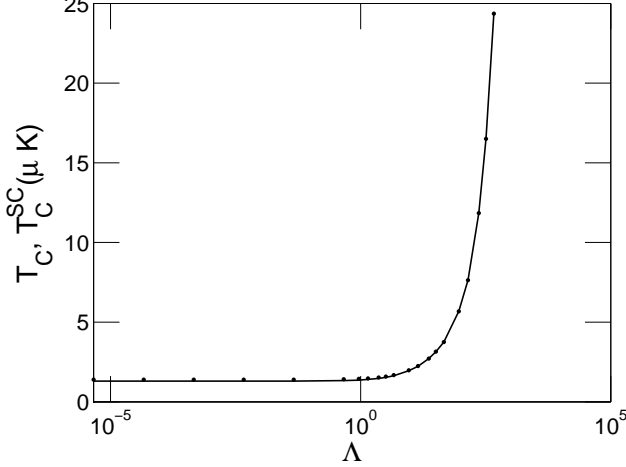


FIG. 1: The critical temperature  $T_c$  and  $T_c^{SC}$  vs  $\Lambda$  for  $N = 10^4$ .  $\Lambda$  is a dimensionless variable defined in Eq. (9). The crosses and dots show  $T_c$  and  $T_c^{SC}$  values, respectively. Here we use  $m = 23$  amu ( $^{23}\text{Na}$ ) and  $\omega = 2\pi \times 21$  Hz [37]. The logarithmic scale is used for  $\Lambda$  axis.

If  $10^8 \text{ 1/m} \leq \sigma \leq 10^{10} \text{ 1/m}$  then  $460 \leq \Lambda \leq 46000$  for the experimental parameters  $m = 23$  amu ( $^{23}\text{Na}$ ),  $\omega = 2\pi \times 21$  Hz [37] and  $230 \leq \Lambda \leq 23000$  for the experimental parameters  $m = 133$  amu ( $^{133}\text{Cs}$ ),  $\omega = 2\pi \times 14$  Hz [21]. In this work, we show that, even for small  $\Lambda$  values, the condensate fraction and critical temperature change considerably.

The critical temperature ( $T_c$ ) is obtained by taking the chemical potential equal to the ground-state energy ( $\mu = E_g = E_0$ ) and

$$N \approx \sum_{i=1}^{\infty} \frac{1}{e^{\beta_c \varepsilon_i} - 1}, \quad (10)$$

at  $T = T_c$ , where  $\beta_c = 1/(k_B T_c)$ . For finite  $N$  value, we define  $T_c^0$  as the solution of Eq. (10) for  $\Lambda = 0$  (only the harmonic trap).

In Eq. (10),  $\varepsilon_i$ 's are the eigenvalues for the potential given in Eq. (7). The energies of odd states are unchanged and equal to  $(2n + 1 + 1/2)\hbar\omega$ . The energies of even states are found by solving Eq. (8) numerically. Then, these values are substituted into the Eq. (10), and finally this equation is solved numerically to find  $T_c$ . We obtain  $T_c$  for different  $\Lambda$  and show our results in Fig. 1. In this figure, logarithmic scale is used for  $\Lambda$  axis. As  $\Lambda$  increases, the critical temperature increases very rapidly when  $\Lambda > 1$ . The solid line in Fig. 1 shows the change of the critical temperature with  $\Lambda$ . Here we take  $N = 10^4$  and use the experimental parameters  $m = 23$  amu ( $^{23}\text{Na}$ ) and  $\omega = 2\pi \times 21$  Hz [37].

We have calculated the change in the critical temperature approximating dimple-type potentials by Dirac  $\delta$  function. The change in the critical temperature can

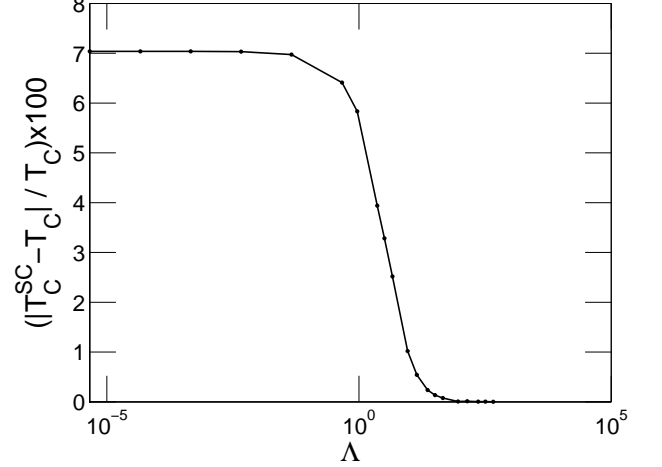


FIG. 2:  $(T_c^{SC} - T_c)/T_c \times 100$  vs  $\Lambda$ , the difference of the critical temperatures calculated by the semiclassical and our method with respect to  $\Lambda$ . The logarithmic scale is used for  $\Lambda$  axis.

also be calculated by assuming that the optical trap is added to harmonic trap adiabatically [20, 38]. In this semi-classical approach, one uses the density of states and assumes the energy spectrum is continuous utilizing the fact that  $\hbar\omega/(k_B T) \ll 1$ . For a one dimensional harmonic trap, the number of particles in the thermal gas can be found as

$$N = N_0 + \frac{1}{\hbar\omega} \int_{(3/2)\hbar\omega}^{\infty} d\varepsilon \frac{1}{e^{\beta(\varepsilon - \mu)} - 1}. \quad (11)$$

where  $N_0$  denotes the average number of particles in the ground state. The  $1/(\hbar\omega)$  factor before the integral in Eq. (11) is the density of states for one dimensional harmonic potential. The critical temperature  $T_c^0$  in the harmonic trap can be found by taking  $\mu = \hbar\omega/2$  and writing the following equation for the total number of particles,  $N$ :

$$N = \frac{1}{\hbar\omega} \int_{(3/2)\hbar\omega}^{\infty} d\varepsilon \frac{1}{e^{\beta_c^0(\varepsilon - \frac{1}{2}\hbar\omega)} - 1}, \quad (12)$$

where  $\beta_c^0 = 1/(k_B T_c^0)$ . The addition of an attractive dimple potential to the harmonic trap decreases the ground-state energy, resulting a decrease in the chemical potential. Since the chemical potential is assumed to be equal to the ground state energy at critical temperature, replacing  $\mu$  in Eq. (11) by  $E_g$ , the ground state energy for the harmonic trap together with the dimple potential, it is possible to calculate the critical temperature of the new system;

$$N = \frac{1}{\hbar\omega} \int_{(3/2)\hbar\omega}^{\infty} d\varepsilon \frac{1}{e^{\beta_c^{SC}(\varepsilon - E_g)} - 1}. \quad (13)$$

where  $\beta_c^{SC} = 1/(k_B T_c^{SC})$  denotes the critical temperature values obtained by semiclassical method. Here we

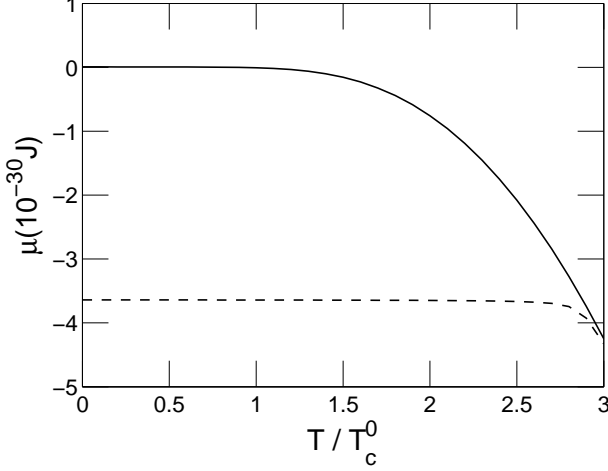


FIG. 3: The chemical potential  $\mu$  vs temperature  $T/T_c^0$  for  $N = 10^4$  and solid line for  $\Lambda = 0$  and dashed line for  $\Lambda = 46$ . The other parameters are the same as Fig. 1.

assume that the energies of the excited state are same with the harmonic trap by following Ref. [20]. We have calculated the critical temperature for various dimple potentials differing according to potential depths. We take the  $E_g$  values as the ground state of the potential given in Eq. (7) for different  $\sigma$  [ or  $\Lambda = \sigma\sqrt{\hbar/(m\omega)}$  ] values in order to compare the results of this method with our results.

The critical temperature values calculated using this semiclassical approach ( $T_c^{SC}$ ) is shown in Fig. 1 as points. As seen from the figure, the critical temperature values estimated by our method and by the semiclassical method are almost equal. We show in Fig. (2) percentage difference of the critical temperatures that are calculated by using these methods. The difference of these two methods for very small  $\Lambda$  values is due to the accurate calculation of the summation with accurate energy values for the excited states for our method; however, the summation is approximated with an integral by using the harmonic trap density of states for the semiclassical method.

For a gas of  $N$  identical bosons, the chemical potential  $\mu$  is obtained by solving

$$N = \sum_{i=0}^{\infty} \frac{1}{e^{\beta(\varepsilon_i - \mu)} - 1} = N_0 + \sum_{i=1}^{\infty} \frac{1}{e^{\beta(\varepsilon_i - \mu)} - 1}, \quad (14)$$

at constant temperature and for given  $N$ , where  $\varepsilon_i$  is the energy of state  $i$ . We present the change of  $\mu$  as a function of  $T/T_c^0$  in Fig.3 for  $N = 10^4$ ;  $\Lambda = 0$  and  $\Lambda = 46$ . By inserting  $\mu$  values into the equation

$$N_0 = \frac{1}{e^{\beta(\varepsilon_0 - \mu)} - 1}, \quad (15)$$

we find the average number of particle in the ground

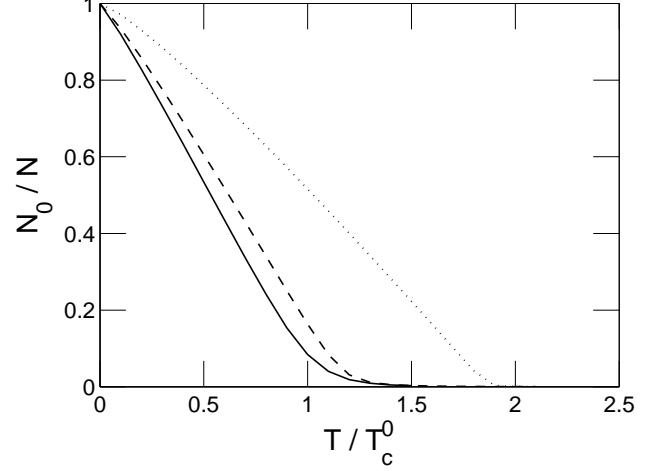


FIG. 4:  $N_0/N$  vs  $T/T_c^0$  for  $N = 10^6$  and solid line for  $\Lambda = 0$ , dashed line for  $\Lambda = 4.6$ , dotted line for  $\Lambda = 46$ . The other parameters are the same as in Fig. 1.

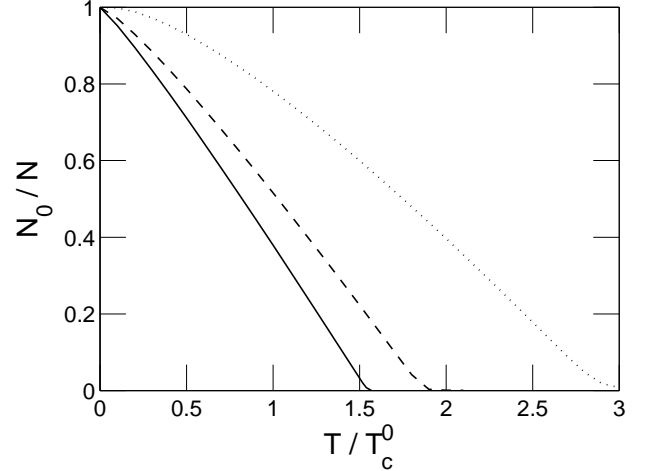


FIG. 5: Condensate  $N_0/N$  vs temperature  $T/T_c^0$  for  $\Lambda = 46$ . The solid line for  $N = 10^8$ , dashed line for  $N = 10^6$ , dotted line for  $N = 10^4$ . The other parameters are the same as in Fig. 1.

state.  $N_0/N$  versus  $T/T_c^0$  for  $N = 10^6$  and  $\Lambda = 0, 4.6, 46$  are shown in Fig. 4. In this figure, the result for  $\Lambda = 0$  is the same as the result obtained by Ketterle and van Druten [8]. As mentioned in Ref. [8], the phase transitions due to discontinuity in an observable macro parameter occurs only in thermodynamic limit, where  $N \rightarrow \infty$ . However, we make our calculations for a realistic system with a finite number of particles. Thus,  $N_0/N$  is a finite nonzero quantity for  $T < T_c$  without having any discontinuity at  $T = T_c$ .

It is useful to know the behavior of the condensate frac-

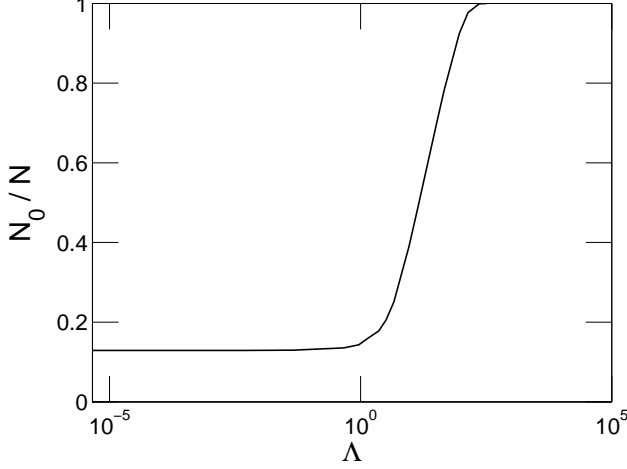


FIG. 6: Condensate fraction  $N_0/N$  vs the strength of the Dirac  $\delta$  potential  $\Lambda$  when  $N = 10^4$ . The logarithmic scale is used for the  $\Lambda$  axis. The other parameters are the same as in Fig. 1.

tion as a function of temperature for a fixed value of  $\Lambda$ . We present the condensate fraction for  $N = 10^4, 10^6, 10^8$  when  $\Lambda = 46$  in Fig. 5. All condensate fractions for different  $N$  values are drawn by using their corresponding  $T_c^0$  values. These  $T_c^0$  values are  $13 \mu\text{K}$  for  $N = 10^4$ ,  $85 \mu\text{K}$  for  $N = 10^6$  and  $6200 \mu\text{K}$  for  $N = 10^8$ .

We also find the condensate fraction as a function of  $\Lambda$  at a constant  $T = T_c^0$ . These results for  $N = 10^4$  are shown in Fig. 6. In the following section we show that the condensate fraction changes exponentially for large  $\Lambda$ . Thus, large  $\Lambda$  values ( $\Lambda > 1$ ) induce sharp increase in the condensate fraction.

Finally, we compare the density profiles of condensates for a harmonic trap and a harmonic trap decorated with a  $\delta$  function ( $\Lambda = 4.6$ ) in Fig. 7. Since the ground-state wave functions can be calculated analytically for both cases, we find the density profiles by taking the absolute square of the ground-state wave functions.

#### IV. ADIABATIC CONDENSATION

One can also find the condensate fraction assuming a dimple potential is added to harmonic trap adiabatically [20, 38]. We first calculate the grand potential of a one-dimensional Bose-gas in a harmonic trap using semi-classical approximation:

$$\Omega = \Omega_0 + \frac{k_B T}{\hbar \omega} \int_{(3/2)\hbar\omega}^{\infty} d\varepsilon \ln \left[ 1 - e^{\beta(\mu - \varepsilon)} \right] \quad (16)$$

where  $\Omega_0$  denotes the contribution of the ground state to the grand potential. The  $1/(\hbar\omega)$  factor before the integral in Eq. (16) is the density of states for one-

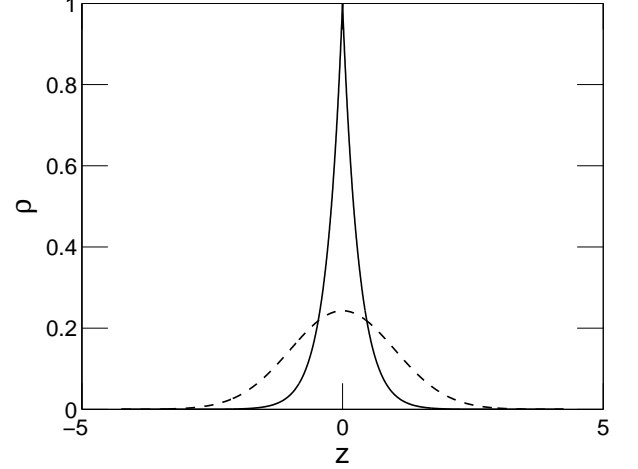


FIG. 7: Comparison of density profiles of a BEC in a harmonic trap with a BEC in a harmonic trap decorated with a  $\delta$  function ( $\Lambda = 4.6$ ). The solid curve is the density profile of the BEC in decorated potential. The dashed curve is the density profile of the 1D harmonic trap ( $\Lambda = 0$ ). The parameter  $z$  is dimensionless length defined after Eq. (2). The other parameters are the same as in Fig. 1.

dimensional harmonic potential. We calculate the entropy using  $S = -d\Omega/dT$  and get

$$\frac{S}{k_B} = \frac{2k_B T}{\hbar \omega} g_2 \left( e^{\beta(\mu - \frac{3}{2}\hbar\omega)} \right) + \left( \frac{\mu}{\hbar \omega} - \frac{3}{2} \right) \ln \left[ 1 - e^{\beta(\mu - 3\hbar\omega/2)} \right]. \quad (17)$$

where  $g_2(x)$  is a Bose function and is defined as

$$g_2(x) = \sum_{l=1}^{\infty} \frac{x^l}{l^2}. \quad (18)$$

For temperatures slightly above  $T_c^0$ , the entropy is

$$\frac{S}{k_B} = \frac{2k_B T}{\hbar \omega} g_2 \left( e^{\frac{\hbar\omega}{k_B T_c^0}} \right) - \ln \left[ 1 - e^{-\frac{\hbar\omega}{k_B T_c^0}} \right], \quad (19)$$

assuming  $\mu = \hbar\omega/2$ . We assume that adding a dimple potential changes the ground state and the chemical potential such that  $\mu = E_g < \hbar\omega/2$  and the entropy expression becomes

$$\frac{S}{k_B} = \frac{2k_B T}{\hbar \omega} g_2 \left( e^{\beta(E_g - \frac{3}{2}\hbar\omega)} \right) + \left( \frac{E_g}{\hbar \omega} - \frac{3}{2} \right) \ln \left[ 1 - e^{\beta(E_g - 3\hbar\omega/2)} \right]. \quad (20)$$

Since the entropy remains constant during an adiabatic process, we can use Eqs. (19) and (20) to calculate the final temperature of the system. Then, we calculate

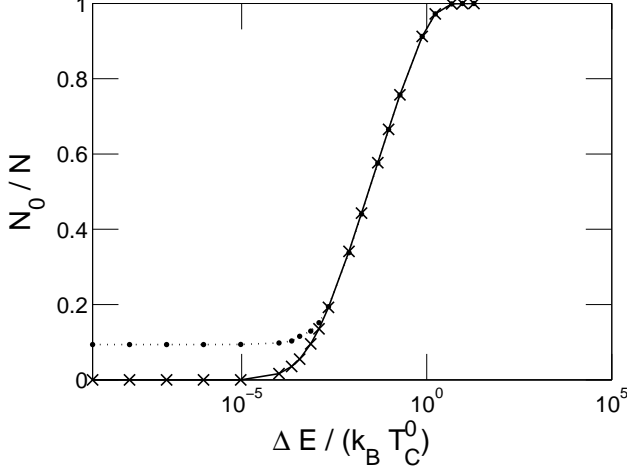


FIG. 8: The comparison of the condensate fraction values evaluated with the semiclassical method and our method for  $N = 10^4$ . The crosses and dots show the results of the semiclassical method and our method, respectively. The logarithmic scale is used for the x axis, where  $\Delta E = \hbar\omega/2 - E_g$ .

the condensate fraction for this final temperature. We present the change of condensate fraction with respect to  $\Delta E / (k_B T_c^0)$  in Fig. 8 where  $\Delta E = \hbar\omega/2 - E_g$ . The solid and dashed lines in Fig. 8 show the results of the semiclassical method and our method, respectively.  $\Delta E$  increases with  $\Lambda$ , representing the potential depth for a constant width. We have calculated the condensate fraction for the same ground-state energy values of the dimple potential in both the semiclassical and our method to make a comparison. The condensate fraction results in Fig. 8 differ for these two methods for very small  $\Lambda$  values. This is due to two effects: (a) Calculations of the chemical potential is done accurately by using the constant  $N$  for the *finite* number of particles for our method, however the chemical potential is just taken the ground-state energy for the semiclassical method [20, 38]. (b) An accurate summation calculation is performed for our method; however, the summation is approximated by an integral for the semiclassical method.

The plots in Figs. 1 and 8 show that the agreement of the results of two methods is better for large  $\Lambda$  (or large  $\Delta E$ ) values. This is due to the fact that the average occupations for excited states is so low ( $n^{excited} \ll 1$ ) that the semiclassical treatment for this gas is valid.

## V. APPROXIMATE SOLUTIONS OF THE CRITICAL TEMPERATURE AND CONDENSATE FRACTION FOR LARGE $\sigma$

If we apply a deep dimple potential ( $\sigma \rightarrow \infty$ ) to the atomic condensate in a harmonic trap, the problem can be solved analytically by approximating the summation

for  $N$  with an integral. As  $T \rightarrow T_c$ ,  $\mu \rightarrow \varepsilon_0 \approx E_\delta$ , where

$$E_\delta = -\frac{\hbar^2}{2m} \left(\frac{\sigma}{2}\right)^2 \quad (21)$$

and it is the bound state energy of a Dirac  $\delta$  potential [32]. By using density of states  $\rho(\varepsilon)$  and utilizing  $E_{2n+2} \rightarrow E_{2n+1}$  (odd-state energies) as  $\sigma \rightarrow \infty$ , the summation in Eq. (14) is converted to the following integral

$$N = \frac{1}{\hbar\omega} \int_{(3/2)\hbar\omega}^{\infty} \frac{d\varepsilon}{e^{\beta_c \varepsilon + \alpha} - 1} \quad (22)$$

where  $\alpha = \beta_c (\hbar^2 / (2m)) (\sigma/2)^2$  and  $\beta_c = 1 / k_B T_c$ . After calculating the integral, we get

$$N = -\frac{k_B T_c}{\hbar\omega} \ln \left( 1 - \exp \left\{ -\beta_c \left[ \frac{3\hbar\omega}{2} - \frac{\hbar^2}{2m} \left(\frac{\sigma}{2}\right)^2 \right] \right\} \right). \quad (23)$$

Defining  $A = |E_\delta| / \hbar\omega$ , we have  $A \gg 1$  and  $\exp(-\beta_c \hbar\omega A) \ll 1$  for very large  $\sigma$ . Then,

$$N \approx \frac{k_B T_c}{\hbar\omega} e^{-\beta_c \hbar\omega A} \quad (24)$$

for this case and we get for the critical temperature

$$k_B T_c \approx \frac{A}{\ln(A/N)} \hbar\omega. \quad (25)$$

for large  $A/N$  value. For one-dimensional experimental systems,  $N \approx 10^3 - 10^6$  atoms. For a specific case  $A/N \approx 10^4 \approx e^9$ , one gets

$$k_B T_c \approx \frac{|E_\delta|}{7}, \quad (26)$$

which shows that the critical temperature increases linearly with increasing bound-state energy for the dimple potential.

By using Eq. (24), the condensate fraction can be written as

$$\frac{N_0}{N} = 1 - \frac{T}{T_c} e^{-\beta \beta_c k_B (T_c - T) \hbar\omega A} \quad (27)$$

for  $T < T_c$ . This result indicates an exponential increase of  $N_0$  as a function of  $T$  for  $T < T_c$ . Thus, the number of atoms in Bose-Einstein condensate will rise drastically when a very strong, very short-range (point) interaction is added to a harmonic confining potential. However, we ignore the interactions between the atoms and neglect nonlinear terms in the Gross-Pitaevski equation which will modify these results.

## VI. CONCLUSION

We have investigated the effect of the tight dimple potential on the harmonically confined one-dimensional

BEC. We model the dimple potential with the Dirac  $\delta$  function. This allows for analytical expressions for the eigenfunctions of the system and a simple eigenvalue equation greatly simplifying numerical treatment. Pure analytical results are obtained in the limit of infinitely deep dimple potential case.

We have calculated the critical temperature, chemical potential and condensate fraction and demonstrated the effect of the dimple potential. We have found that the critical temperature can be enhanced by an order of magnitude for experimentally accessible dimple potential parameters. In general,  $T_c$  increases with the relative strength of the dimple potential with respect to the harmonic trap. In our model system, the increase in the strength of the Dirac  $\delta$  function can be interpreted as increasing the depth of a dimple potential.

In addition, the change of the condensate fraction with respect to the strength of the Dirac  $\delta$  function has been analyzed at a constant temperature ( $T = T_c^0$ ) and with respect to temperature at a constant strength. It has been shown that the condensate fraction can be increased considerably and large condensates can be achieved at higher temperatures due to the strong localization effect of the dimple potential. Analytical expressions are given to clarify the relation of the condensate fraction and critical temperature to the strength of deep dimple potential.

We also show that similar results for the critical temperature and condensate fraction can be obtained by us-

ing a semiclassical approximation. However, in this simpler approach, it is not possible to determine the density profile and when the thermodynamic limit is not satisfied, the estimations of semiclassical approach fail.

Finally, we have determined and compared the density profiles of the harmonic trap and the decorated trap with the Dirac  $\delta$  function at the equilibrium point using analytical solutions of the model system. Comparing the graphics of density profiles, we see that a dimple potential maintains a considerably higher density at the center of the harmonic trap.

The results presented are obtained for the case of non-interacting condensates for simplicity. The treatment should be extended to the case of interacting condensates in order to make the results more relevant to experimental investigations. This case deserves further detailed and separate calculations. We believe the method presented of  $\delta$ -function modelling of tight dimple potentials can help significantly such theoretical examinations.

### Acknowledgments

O.E.M. acknowledges support from a TÜBA/GEPIB grant. E.D. is supported by Turkish Academy of Sciences, in the framework of the Young Scientist Program (ED- TÜBA- GEPIB-2001-1-4).

- 
- [1] A. Einstein, Sitzungsber. Preuss Akad. Wissen., Physik.-Mathem. Klasse p. 261 (1924); *ibid* p. 3 (1925).
  - [2] S. N. Bose, Z.Phys **26** 178 (1924).
  - [3] A. Einstein's letter to P. Ehrenfest in A. Pais, *Subtle is the Lord* (Oxford University Press, New York, 2005)
  - [4] M. H. Anderson, J. R. Ensher, M. R. Matthews, C. E. Wieman, and E. A. Cornell, Science **269** 198 (1995).
  - [5] C. C. Bradley, C. A. Sackett, J. J. Tollett, and R. G. Hulet, Phys. Rev. Lett. **75** 1687 (1995).
  - [6] K. B. Davis, M.-O. Mewes, M. R. Andrews, N. J. van Druten, D. S. Durfee, D. M. Kurn, and W. Ketterle, Phys. Rev. Lett. **75** 3969 (1995).
  - [7] F. London, Phys. rev. **54**, 947 (1938).
  - [8] W. Ketterle and N. J. van Druten, Phys. Rev. A **54** 656 (1996).
  - [9] N. J. van Druten and W. Ketterle, Phys. Rev. Lett. **79** 549 (1997).
  - [10] U. Al Khawaja, J. O. Andersen, N. P. Proukakis, and H. T. C. Stoof, Phys. Rev. A **66** (2002).
  - [11] D. S. Petrov, G. V. Shlyapnikov, J. T. M. Walraven, Phys. Rev. Lett. **85**, 3745 (2000).
  - [12] S. R. de Groot, G. J. Hooyman, and C. A. ten Seldam, Proc. R. London Ser. A **203**, 266 (1950).
  - [13] N. D. Mermin and H. Wagner, Phys. Rev. Lett. **17**, 1133 (1966).
  - [14] P. C. Hohenberg, Phys. rev. **158**, 383 (1967).
  - [15] A. Görlitz, J. M. Vogels, A. E. Leanhardt, C. Raman, T. L. Gustavson, J. R. Abo-Shaer, A. P. Chikkatur, S. Gupta, S. Inouye, T. Rosenband, and W. Ketterle, Phys. Rev. Lett. **87**, 130402 (2001).
  - [16] H. Ott, J. Fortagh, G. Schlotterbeck, A. Grossmann, and C. Zimmermann, Phys. Rev. Lett. **87**, 230401 (2001).
  - [17] W. Hänsel, P. Hommelhoff, T. W. Hansch, and J. Reichel, Nature (London) **413**, 501 (2001).
  - [18] F. Schreck, L. Khaykovich, K. L. Corwin, G. Ferrari, T. Bourdel, J. Cubizolles, and C. Salomon, Phys. Rev. Lett. **87**, 080403 (2001).
  - [19] P. W. H. Pinkse, A. Mosk, M. Weidemüller, M. W. Reynolds, T. W. Hijmans, and J. T. M. Walraven, Phys. Rev. Lett. **78** 990 (1997).
  - [20] D. M. Stamper-Kurn, H.-J. Miesner, A. P. Chikkatur, S. Inouye, J. Stenger, W. Ketterle, Phys. Rev. Lett. **81** 2194 (1998).
  - [21] T. Weber, J. Herbig, M. Mark, H.-C. Nägerl, and R. Grimm, Science **299** 232 (2003).
  - [22] Z.-Y. Ma, C. J. Foot, S. L. Cornish, J. Phys. B **37** 3187 (2004).
  - [23] D. Comparat, A. Fioretti, G. Stern, E. Dimova, B. Laburthe-Tolra, and P. Pillet, Phys. Rev. A **73** 043410 (2006).
  - [24] N. G. Parker, N. P. Proukakis, M. Leadbeater, and C. S. Adams, Phys. Rev. Lett. **90**, 220401 (2003).
  - [25] D. Jaksch and P. Zoller, Annals of Physics **315**, 52 (2005).
  - [26] R. B. Diener, B. Wu, M. G. Raizen, and Q. Niu, Phys. Rev. Lett. **89**, 070401 (2002).
  - [27] P. F. Griffin, K. J. Weatherill, S. G. Macleod, R. M. Potvliege, and C. S. Adams, New Jour. Phys. **8**, 11 (2006).

- [28] N. P. Proukakis, J. Schmiedmayer, and H. T. C. Stoof, Phys. Rev. A **73**, 053603 (2006).
- [29] J. Anglin, Phys. Rev. Lett. **79** 6 (1996)
- [30] M. J. Lighthill, *An introduction to Fourier analysis and generalized functions* (University Press, Cambridge, 1959).
- [31] E. Demiralp, J.Phys.A: Math. Gen. **38** 4783 (2005).
- [32] M.P. Avakian, G. Pogosyan, A.N. Sissakian and V.M. Ter-Antonyan, Phys.Lett.A **124** 233 (1987).
- [33] E. Demiralp, "Properties of One-Dimensional Harmonic Oscillator with the Dirac delta Functions, *Unpublished Notes*.
- [34] N. N. Lebedev, *Special Functions and Their Applications* (Dover Pub., Inc., New York, 1972).
- [35] E. Demiralp and H. Beker, J.Phys.A: Math. Gen. **36** 7449 (2003).
- [36] There is a small numerical error in [32]. The right hand side of Eq. (12) in [32] should be divided by  $2^{3/2}$ .
- [37] L.V. Hau, S.E. Harris, Z. Dutton, and C.H. Behroozi, Nature (London) **397**, 594-598 (1999).
- [38] L. Pitaevskii, S. Stringari, *Bose-Einstein Condensation* (Clarendon Press, Oxford, 2003).